Published in final edited form as:
J Dent Res. 2009 November ; 88(11): 1003–1007. doi:10.1177/0022034509346928.

Osterix Enhances BMSC-associated Osseointegration of Implants

B. Xu[1,2,+], **J. Zhang**[1,+], **E. Brewer**[1], **Q. Tu**[1], **L. Yu**[2], **J. Tang**[1], **P. Krebsbach**[3], **M. Wieland**[4], and **J. Chen**[1,*]

[1] Division of Oral Biology, Tufts University School of Dental Medicine, One Kneeland Street, Boston, MA 02111, USA [2] Department of Stomatology, Huashan Hospital, Fudan University, Shanghai, China [3] Department of Biologic and Materials Sciences, University of Michigan School of Dentistry, Ann Arbor, MI, USA [4] Institute Straumann AG, Basel, Switzerland

Abstract

Cellular and molecular events in osseointegration at the dental implant surface remain largely unknown. We hypothesized that bone marrow stromal cells (BMSCs) participate in this process, and that osterix (Osx) promotes implant osseointegration. To prove this hypothesis, we tracked double-labeled BMSCs in implantation sites created in nude mice transplanted with these cells. We also inserted implants into the femurs of our established transgenic mice after local administration of viruses encoding Osx, to determine the osteogenic effects of Osx. Immunohistochemical results demonstrated that BMSCs can recruit from peripheral circulation and participate in wound healing and osseointegration after implantation. Microcomputed tomography (microCT) analysis revealed an increased bone density at the bone-to-implant interface in the Osx group, and histomorphometric analysis indicated an elevated level of bone-to-implant contact in the Osx group. We concluded that exogenous BMSCs participate in the osseointegration after implantation, and that Osx overexpression accelerates osseointegration.

Keywords

implant; osterix; bone marrow stromal cells; cell recruitment; stem cells; bone regeneration; osseointegration; mice

INTRODUCTION

Although the insertion of dental implants has become a standard procedure, osseointegration at the dental implant surface still remains a challenge. It is widely accepted that the recruitment and differentiation of osteoprogenitor cells, which are from neighboring host tissues (Seo *et al.*, 2004), are the key to bone regeneration after dental implantation (Fuerst *et al.*, 2003; Schneider *et al.*, 2004; Mannai, 2006). However, it is also known that the population of mesenchymal cells with osteogenic potential is limited in the vicinity of dental implants, which may explain why bone regeneration around implants is relatively slow. This raises questions of how we can accelerate osteogenesis by finding new sources of cells and recruit more cells from other channels using modern cell and molecular approaches.

*corresponding author, jk.chen@tufts.edu.
+authors contributing equally to this work;

A supplemental appendix to this article is published electronically only at http://jdr.sagepub.com/supplemental.

Bone marrow stromal cells (BMSCs) contain a subset of mesenchymal stem cells that maintain multipotential, differentiative features (Nussenbaum and Krebsbach, 2006; Robey and Bianco, 2006). Using human BMSCs, we successfully regenerated bone in calvarial defects (Meinel *et al.*, 2005; Karageorgiou *et al.*, 2006). We also provided the first evidence showing that osteoblast progenitors are recruited from bone marrow and access bone regeneration sites from peripheral circulation (Li *et al.*, 2008). However, there is no convincing evidence showing that bone-marrow-derived osteoprogenitor cells migrate to the dental implantation sites and adhere to the surfaces of dental implants.

In 2002, a new transcription factor, osterix (Osx), was discovered and characterized (Nakashima *et al.*, 2002). In Osx null mice, no bone formation occurs, and cells in the periosteum and the membranous skeletal elements cannot differentiate into osteoblasts. In a recently published *in vivo* study, we found that there was increased new bone formation in the wound sites where Osx was applied, as compared with controls (Tu *et al.*, 2007). These results are the first demonstration that Osx may function during bone regeneration to control the differentiation of cells involved in the regenerative process.

To investigate further the molecular and cellular mechanisms underlying osseointegration after dental implantation, we transplanted double-labeled BMSCs into nude mice through intracardiac injection and traced the cells using immuno-histochemical staining. We also used Osx to enhance the differentiation of bone-forming cells to accelerate osseointegration of dental implants.

MATERIALS & METHODS

BMSCs Transplantation and Implant Placement

As described previously, BMSCs were obtained from 7-week-old BSP-Luc/ACTB-EGFP mice and were cultured under non-differentiating conditions (DMEM with 10% fetal bovine serum, 100 mg/mL penicillin, and 100 mg/mL streptomycin) (Li *et al.*, 2008). These BMSCs were genetically double-labeled with a luciferase reporter gene driven by bone sialoprotein (BSP) promoter and an enhanced green fluorescent protein (EGFP) driven by a beta-actin promoter (Li *et al.*, 2008). Five wks after intracardiac injection of these cells into 4-week-old male nude mice (2×10^6 cells *per* mouse), titanium implants were inserted into the femurs of these recipient mice.

The titanium implants (1 mm in diameter and 2 mm in length, Institute Straumann AG, Basel, Switzerland) had a machined surface. The surface mean roughness value, Sa, was 0.3 ± 0.06 mm, measured with white light confocal microscopy. The measurement area was 798 mm × 770 mm. Briefly, for the surgical procedure, the implant sites were prepared on anterior-distal surfaces of the femurs by sequential drilling under cooled sterile saline irrigation with 0.4-, 0.5-, and 0.7-mm surgical stainless steel twist drills. Then the implants were press-fitted into slightly undersized holes. After the insertion of the implant, the muscles were carefully sutured, which covered the implant and further guaranteed the stability of the implant. The animals were killed at 7 and 21 days after surgery.

All mice in this study were maintained in accordance with recommendations in the Guide for the Care and Use of Laboratory Animals prepared by the Institute on Laboratory Animal Resources, National Research Council (DHHS Publ. NIH 86-23, 1985), and by guidelines established by the Institutional Animal Care and Use Committee of the Tufts Medical Center in Boston, MA.

Local Application of RCAS/Osx in BSP-TVA Mice and Placement of Implants

To investigate the effect of Osx in promoting osseointegration after implantation, we prepared replication-competent avian retroviruses (RCAS) as previously described (Tu *et al.*, 2006). A 5-μL quantity of RCAS-Osx or RCAS-vector control (10^8 cfu/mL) was applied to the bone defects in the femurs of 3- to 4-month-old BSP-TVA mice, in which the avian retroviral *receptor TVA*, driven by a BSP promoter, was selectively expressed in osteogenic cells (Li *et al.*, 2005). Then the above-mentioned titanium implants were inserted. The femurs were isolated 7 and 14 days after surgery.

Histomorphometric Analysis

The femoral samples were fixed in 10% neutral-buffered formalin solution for 7 days. After decalcification, the implants were gently removed, and the tissues were dehydrated in an ascending series of ethanol, cleared in xylene, and embedded in paraffin. Tissue sections, 6 μm in thickness, were mounted on glass slides. Histomorphometric analysis was performed on H&E-stained sections. The images were taken under a Nikon Eclipse E600 microscope. The newly formed bone area, which was restricted to the 0.5-mm area surrounding the implant, was determined with Spot Advanced Software (Diagnostic Instruments, Sterling Heights, MI, USA). In addition, the percentage of new bone edges in direct contact with the implant surface was determined.

Immunohistochemical (IHC) Staining

Immunohistochemical staining was performed by means of a Histostaining kit (Zymed Laboratories Inc., South San Francisco, CA, USA) as previously described (Paz *et al.*, 2005). Primary antibodies against firefly luciferase (Santa Cruz Biotechnology, Inc., Santa Cruz, CA, USA), GFP (Clontech, Palo Alto, CA, USA), and BSP (a gift from Dr. Larry Fisher, NIH/NIDCR) were used. Positive controls were bone tissue sections derived from our transgenic mice BSP-Luc/ACTB-EGFP double-labeled with luciferase and EGFP (Li *et al.*, 2008). Negative controls were tissue sections incubated with an irrelevant antibody (anti-human CD4 lymphocyte antigen). Stained slides were observed under the Nikon Eclipse E600 microscope, and cell counts were performed with an intra-ocular grid (250 μm × 250 μm). The numbers of BSP-, GFP-, and luciferase-positive cells were normalized to the total number of cells at the implant-bone interface (Li *et al.*, 2008).

MicroCT Scanning

Following fixation, femurs with implants were scanned by micro-computed tomography (Siemens Inveon MicroCT System, Bensheim, Germany). The dose for scanning was 205 mR/mAs at 80 kVp, and the time range for microCT scanning and reconstruction was 60 min, so that high-resolution images (35 μm) could be acquired. According to the histomorphometric measurements on H&E-stained sections, the newly formed bone was restricted to a 0.5-mm area surrounding the implant. Thus, at a 3D level, the Hounsfield Unit (HU) of this newly formed bone area was determined with eFilm Workstation 2.12 (Merge Technologies Inc., Milwaukee, WI, USA).

Reverse-transcription Polymerase Chain-reaction (RT-PCR) Analysis

The femoral bone tissues bordering the implant (1 mm mesial and distal to the implantation site) were dissected without the overlying soft tissues. The bone tissues were snap-frozen in liquid nitrogen as previously described (Chikazu *et al.*, 2007), and the implant was carefully removed. Total RNA was extracted from the bone tissues with the use of TRIzol reagent (Invitrogen, Carlsbad, CA, USA), reverse-transcribed with a SuperScript first-strand synthesis system (Invitrogen), and then amplified with Platinum PCR supermix (Invitrogen). The sequences of the primers for amplification of mouse Osx, BSP, osteocalcin (OC), and GAPDH

were as reported previously (Tu *et al.*, 2006). Images of the amplified products in 1.2% agarose gels were captured by means of a UVP bioimaging system (UVP, Upland, CA, USA) and processed by Scion Image Beta 4.02 (Scion Corp., Frederick, MD, USA).

Statistical Analysis

Raw data were expressed as means ± SEM of 3 or more independent experiments. We used one-way ANOVA to test significance using the software package Origin 6.1 (Origin Lab, Northampton, MA, USA). Values of $p < 0.05$ were considered statistically significant.

RESULTS

Transplanted Double-labeled BMSCs Participated in Osseointegration after Implantation

New bone formation was activated 7 days after placement of the implant. Three wks after implantation, the newly formed woven bone had been replaced by lamellar bone. MicroCT analysis showed that, 21 days after implantation, implants were successfully integrated with the host bone tissues. However, the bone mineral density of the newly formed bone was still lower than that of the host bone (Appendix Fig.). Immunohistochemical staining demonstrated that, 7 days after surgery, luciferase, BSP, and GFP activity could be detected in the newly formed bone area. Three wks after surgery, expressions of luciferase, BSP, and GFP were much weaker (Fig. 1A). Cell-counting results showed that, 7 days after implantation, GFP-positive cells (total transplanted BMSCs) constituted 62.5% of the cell population. This percentage decreased slightly thereafter to 59.4% (Fig. 1C). As demonstrated by the percentage of luciferase-positive cells compared with GFP-positive cells, 88.9% of transplanted BMSCs were undergoing osteogenic differentiation 7 days after surgery, and this percentage decreased to 26% 21 days after implantation. Similarly, the percentage of BSP-positive cells decreased from 78.6% at 7 days post-operatively to 24.3% at 21 days post-operatively (Fig. 1B).

Osx Administration Increased the Density of the Newly Formed Bone Surrounding the Implant

MicroCT analysis demonstrated that, 14 days after implantation, implants were successfully integrated with the host bone tissues in both the Osx group and the control group (Fig. 2A). However, the density of the newly formed bone surrounding the implant was higher in the Osx group than in the control group (Fig. 2B).

Local Administration of RCAS/Osx Enhanced New Bone Formation after Implantation

Histological analysis revealed that active osteoblasts appeared at the bone-to-implant interface and new bone was formed 7 days after implantation. The amount of newly formed bone was significantly increased at day 14 in both groups. Histomorphometric analysis indicated that the newly formed bone area was significantly higher in the RCAS/Osx group (63.78%) than in the control group (54.81%) 14 days after implantation. The percentage of new bone edges in direct contact with the implant was also increased in the RCAS/Osx group (Fig. 3).

RT-PCR Analysis

Semi-quantitative RT-PCR analysis showed that, at 7 days post-operatively, levels of Osx, BSP, and OC were significantly higher in the Osx group than in the control group (Fig. 4). At 14 days post-operatively, levels of BSP and OC were higher in the Osx group when compared with the control group. In addition, levels of Osx, BSP, and OC in both the Osx group and the control group were higher 14 days than 7 days post-operatively.

DISCUSSION

Although work has been done to enhance bone-implant integration, osseointegration at the dental implant surface still remains a challenge, partly due to the scarcity of bone-forming cells in the dental implant insertion site. This poses difficulty in early placement and immediate loading and thus limits the use of dental implants in certain individuals. BMSCs are adherent cells of non-hematopoietic origin that are capable of self-renewal and can differentiate into several phenotypes, including bone, cartilage, and adipocytes (Owen, 1988; Pereira *et al.*, 1995; Bruder *et al.*, 1997). Under optimal culture conditions, billions of BMSCs can be generated from a limited amount of starting material (Krebsbach *et al.*, 1998), and *in vitro*-expanded BMSCs are a rich source of osteoprogenitor cells, which can promote the regeneration of skeletal defects. Although we have provided the first evidence that osteoprogenitors are recruited from bone marrow and access sites of bone regeneration from peripheral circulation (Li *et al.*, 2008), it remains unclear whether systemically delivered BMSCs participate in bone-implant integration.

In this study, the BMSC donor mice were genetically double-labeled by 2 reporter genes. First, the luciferase gene was driven by a mouse BSP promoter, serving as a faithful and sensitive marker for osteogenic differentiation of the transplanted BMSCs (Paz *et al.*, 2005). Second, the GFP gene driven by an actin promoter and cytomegalovirus enhancer facilitated the easy identification of transplanted BMSCs from the host cells. This powerful tool enabled us to investigate the process of cell aggregation and subsequent bone apposition on the dental implants. Our results provided the first convincing evidence that transplanted BMSCs can be recruited from circulation to the implantation sites in response to long-range signals originating from the surgical wound of implant placement.

Osx is a critical regulator in osteoblast differentiation and bone formation. It acts downstream of Runx2/Cbfa1 to induce differentiation of preosteoblasts into fully functional osteoblasts (Nakashima *et al.*, 2002). Our previous *in vitro* studies showed that RCAS/Osx-transduced BMSCs were able to form bone nodules in the absence of any other osteogenic factors in the culture media. Furthermore, Osx could enhance the *in vitro* proliferation and osteogenic lineage commitment of BMSCs (Tu *et al.*, 2006). In this study, to address the effect of Osx on osseointegration after implantation, we took advantage of a unique TVA transgenic model (BSP-TVA mice) recently established in our lab (Li *et al.*, 2005). The TVA/RCAS retroviral strategy has been applied for over a decade and is considered to provide an alternative delivery system for gene therapy in bone regeneration (Federspiel and Hughes, 1997; Holland and Varmus, 1998). In BSP-TVA mice, the TVA receptor driven by a BSP promoter is selectively expressed in osteogenic cells, and Osx overexpression can be achieved in these cells after local administration of RCAS/Osx. As demonstrated by RT-PCR analysis, the RCAS/Osx group showed a 1.6-fold increase in Osx levels when compared with the control group 7 days after surgery. Although no significant difference in Osx expression was detected between the two groups at day 14, expressions of BSP and OC were increased in RCAS/Osx group at both day 7 and day 14, indicating that an early increase in Osx expression can induce prolonged changes in the expression levels of bone matrix proteins. MicroCT and histomorphometric analyses also showed that local administration of RCAS/Osx induced accelerated bone apposition at the implant surface at day 14 as compared with the control group. The results of this study suggest that Osx overexpression at the implantation site enhances osteogenic differentiation and triggers osteoblasts to express bone matrix molecules, which accelerates the bone-remodeling process and increases implant stability.

In conclusion, our results show that exogenous BMSCs participate in osseointegration after implantation. Moreover, locally administered Osx specifically targets BMSCs as well as local stem cells, and the resultant Osx expression promotes osteogenic differentiation, triggers

specific gene expressions of matrix proteins, and subsequently enhances bone regeneration and implant stabilization.

Supplementary Material

Refer to Web version on PubMed Central for supplementary material.

Acknowledgments

This study was supported by Institute Straumann AG, Basel, Switzerland, and JZ, EB, QT, and JC are supported by NIH grant DE16710 to JC.

References

Bruder SP, Jaiswal N, Haynesworth SE. Growth kinetics, self-renewal, and the osteogenic potential of purified human mesenchymal stem cells during extensive subcultivation and following cryopreservation. J Cell Biochem 1997;64:278–294. [PubMed: 9027588]

Chikazu D, Tomizuka K, Ogasawara T, Saijo H, Koizumi T, Mori Y, et al. Cyclooxygenase-2 activity is essential for the osseointegration of dental implants. Int J Oral Maxillofac Surg 2007;36:441–446. [PubMed: 17376655]

Federspiel MJ, Hughes SH. Retroviral gene delivery. Methods Cell Biol 1997;52:179–214. [PubMed: 9379950]

Fuerst G, Gruber R, Tangl S, Sanroman F, Watzek G. Enhanced bone-to-implant contact by platelet-released growth factors in mandibular cortical bone: a histomorphometric study in minipigs. Int J Oral Maxillofac Implants 2003;18:685–690. [PubMed: 14579956]

Holland EC, Varmus HE. Basic fibroblast growth factor induces cell migration and proliferation after glia-specific gene transfer in mice. Proc Natl Acad Sci USA 1998;95:1218–1223. [PubMed: 9448312]

Karageorgiou V, Tomkins M, Fajardo R, Meinel L, Snyder B, Wade K, et al. Porous silk fibroin 3-D scaffolds for delivery of bone morphogenetic protein-2 in vitro and in vivo. J Biomed Mater Res A 2006;78:324–334. [PubMed: 16637042]

Krebsbach PH, Mankani MH, Satomura K, Kuznetsov SA, Robey PG. Repair of craniotomy defects using bone marrow stromal cells. Transplantation 1998;66:1272–1278. [PubMed: 9846508]

Li L, Zhu J, Tu Q, Yamauchi M, Sodek J, Karsenty G, et al. An in vivo model to study osteogenic gene regulation: targeting an avian retroviral receptor (TVA) to bone with the bone sialoprotein (BSP) promoter. J Bone Miner Res 2005;20:1403–1413. [PubMed: 16007338]

Li S, Tu Q, Zhang J, Stein G, Lian J, Yang PS, et al. Systemically transplanted bone marrow stromal cells contributing to bone tissue regeneration. J Cell Physiol 2008;215:204–209. [PubMed: 17960569]

Mannai C. Early implant loading in severely resorbed maxilla using xenograft, autograft, and platelet-rich plasma in 97 patients. J Oral Maxillofac Surg 2006;64:1420–1426. [PubMed: 16916679]

Meinel L, Fajardo R, Hofmann S, Langer R, Chen J, Snyder B, et al. Silk implants for the healing of critical size bone defects. Bone 2005;37:688–698. *erratum* in *Bone* 43:1122, 2008. [PubMed: 16140599]

Nakashima K, Zhou X, Kunkel G, Zhang Z, Deng JM, Behringer RR, et al. The novel zinc finger-containing transcription factor osterix is required for osteoblast differentiation and bone formation. Cell 2002;108:17–29. [PubMed: 11792318]

Nussenbaum B, Krebsbach PH. The role of gene therapy for craniofacial and dental tissue engineering. Adv Drug Deliv Rev 2006;58:577–591. [PubMed: 16766080]

Owen M. Marrow stromal stem cells. J Cell Sci Suppl 1988;10:63–76. [PubMed: 3077943]

Paz J, Wade K, Kiyoshima T, Sodek J, Tang J, Tu Q, et al. Tissue- and bone cell-specific expression of bone sialoprotein is directed by a 9.0 kb promoter in transgenic mice. Matrix Biol 2005;24:341–352. [PubMed: 15970437]

Pereira RF, Halford KW, O'Hara MD, Leeper DB, Sokolov BP, Pollard MD, et al. Cultured adherent cells from marrow can serve as long-lasting precursor cells for bone, cartilage, and lung in irradiated mice. Proc Natl Acad Sci USA 1995;92:4857–4861. [PubMed: 7761413]

Robey PG, Bianco P. The use of adult stem cells in rebuilding the human face. J Am Dent Assoc 2006;137:961–972. [PubMed: 16803822]

Schneider GB, Zaharias R, Seabold D, Keller J, Stanford C. Differentiation of preosteoblasts is affected by implant surface microtopographies. J Biomed Mater Res A 2004;69:462–468. [PubMed: 15127393]

Seo BM, Miura M, Gronthos S, Bartold PM, Batouli S, Brahim J, et al. Investigation of multipotent postnatal stem cells from human periodontal ligament. Lancet 2004;364:149–155. [PubMed: 15246727]

Tu Q, Valverde P, Chen J. Osterix enhances proliferation and osteogenic potential of bone marrow stromal cells. Biochem Biophys Res Commun 2006;341:1257–1265. [PubMed: 16466699]

Tu Q, Valverde P, Li S, Zhang J, Yang P, Chen J. Osterix overexpression in mesenchymal stem cells stimulates healing of critical-sized defects in murine calvarial bone. Tissue Eng 2007;13:2431–2440. [PubMed: 17630878]

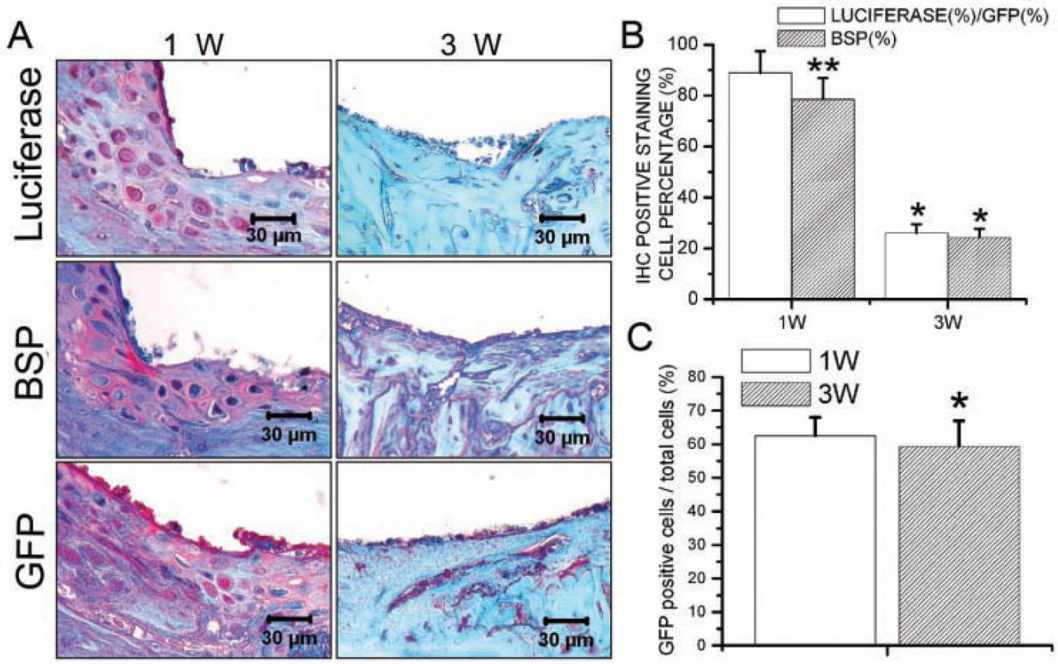

Figure 1.

Transplanted BMSCs participated in osseointegration after implantation. **(A)** Immunohistochemical staining demonstrated that, 7 days after surgery, luciferase, BSP, and GFP activity could be detected in the newly formed bone area. Three wks after surgery, expressions of luciferase, BSP, and GFP were much weaker. **(B)** The percentage of luciferase-positive cells relative to GFP-positive cells, which demonstrated the amount of transplanted BMSCs undergoing osteogenic differentiation, decreased from 88.9% at day 7 to 26% at day 21 after implantation. The percentage of BSP-positive cells also decreased from 78.6% at 7 days post-operatively to 24.3% at 21 days post-operatively. Data are presented as means ± SE (n = 7). *$p < 0.05$, 1w *vs.* 3w; **$p < 0.05$, luciferase (%)/GFP (%) *vs.* BSP (%). (**C**) GFP-positive cells (total transplanted BMSCs) constituted 62.5% of the cell population at day 7 post-operatively. This percentage decreased slightly thereafter to 59.4%. Data are presented as means ± SE (n = 7). *$p < 0.05$, 1w *vs.* 3w.

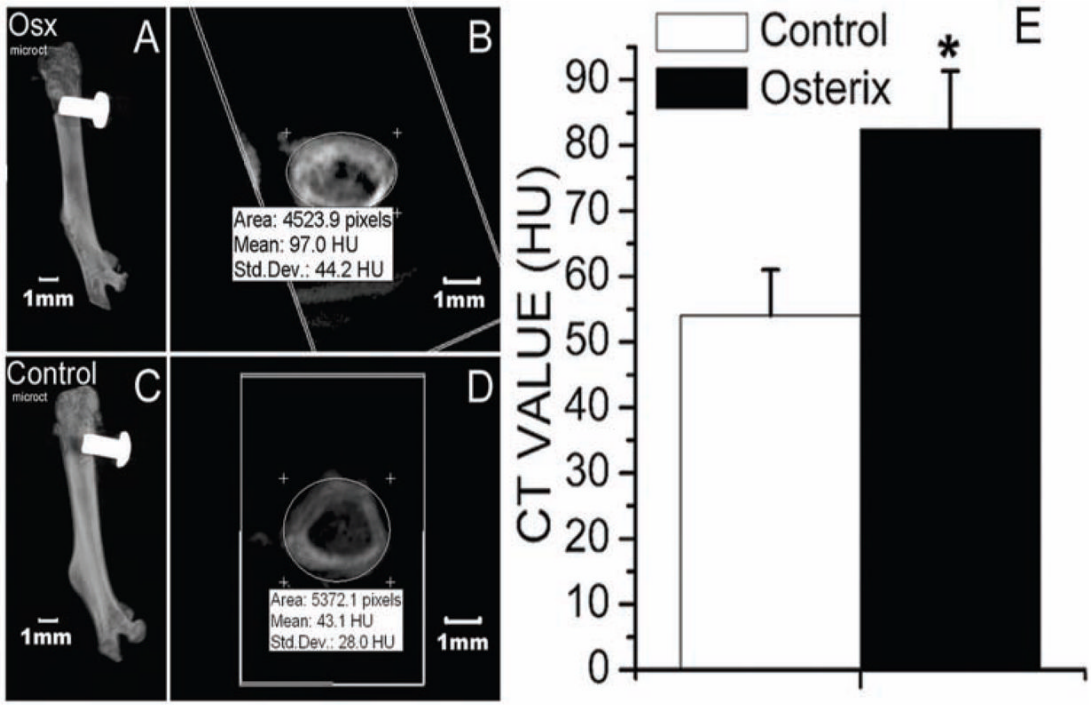

Figure 2.

MicroCT analysis indicated that, 14 days after implantation, implants were successfully integrated with the host bone tissues in both the Osx group **(A)** and the control group **(C).** The CT value of newly formed bone area surrounding the implant in both the Osx **(B)** and control **(D)** groups, demonstrated by Hounsfield Units (HU), was determined by means of the eFilm Workstation 2.12. **(E)** The CT value of the newly formed bone area surrounding the implant was higher in the Osx group than in the control group. Data are presented as means ± SE (n = 8). *$p < 0.05$, Osx group *vs.* control group.

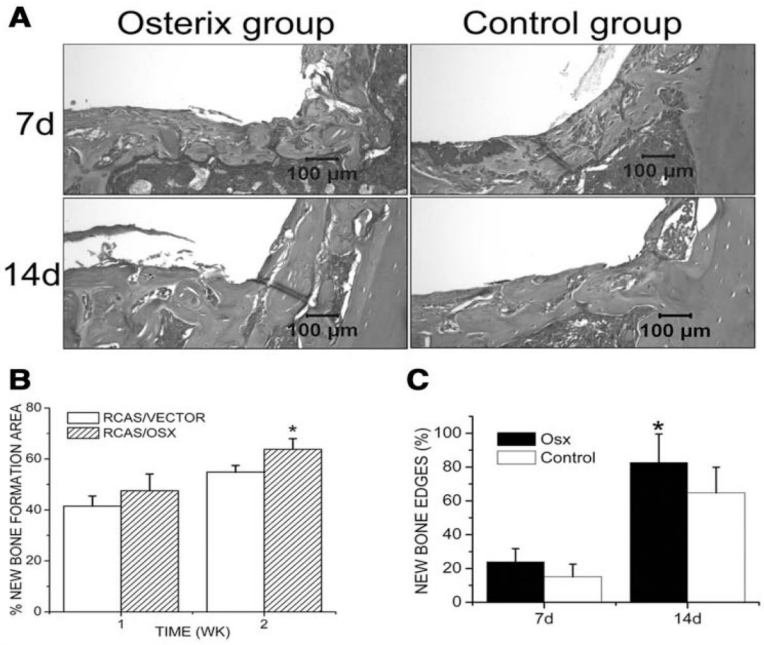

Figure 3.

Histomorphometric analysis. **(A)** H&E-stained tissue sections from different groups. **(B)** The percentages of newly formed bone area at the implantation sites and **(C)** the percentages of new bone edges in direct contact with the implants were determined at day 7 and day 14 post-operatively. Data are presented as means ± SE (n = 8). *p < 0.05, RCAS/VECTOR *vs.* RCAS/OSX.

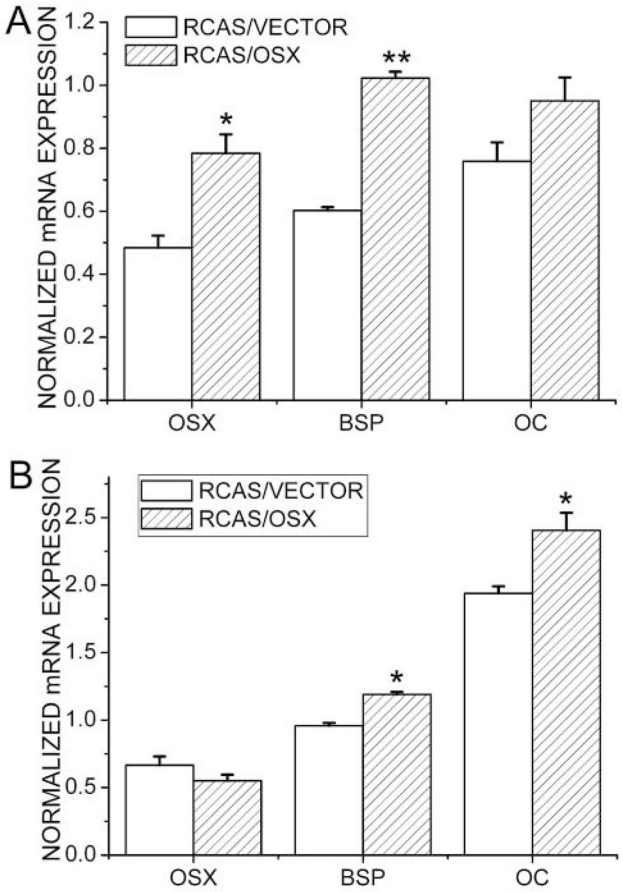

Figure 4.

Semi-quantitative RT-PCR analyses of expression levels of Osx, BSP, and OC. **(A)** Day 7 post-operatively; **(B)** day 14 post-operatively. Data are presented as means ± SE (n = 8). *p < 0.05, **p < 0.01, RCAS/VECTOR *vs.* RCAS/OSX.